The structure of liquid crystalline copolyester fibers prepared from *p*-hydroxybenzoic acid, 2,6-dihydroxy naphthalene, and terephthalic acid

John Blackwell and Genaro Gutierrez
Department of Macromolecular Science, Case Western Reserve University, Cleveland, Ohio 44106, *USA*
(*Received* 29 *June* 1981; *revised* 21 *September* 1981)

X-ray methods are being used to investigate the physical structure of high strength melt-spun liquid crystalline aromatic copolyester fibres prepared from the following monomers: *p*-hydroxybenzoic acid (B), 2,6-dihydroxy naphthalene (N), and terephthalic acid (P). The X-ray data for fibres prepared for B/N/P ratios of 60/20/20, 50/25/25, and 40/30/30 show variations in the positions and intensities of the maxima suggestive of a truly random copolymer structure rather than extensive block copolymer character. We have predicted the intensity distribution on the meridian of the X-ray patterns by modelling random chains by a linear sequence of points separated by distances corresponding to the lengths of the B, N and P residues. The positions of the maxima in the averaged squared Fourier transforms of random monomer sequences are in good agreement with those for the three observed strong meridional intensities, and the calculations reproduce the observed shifts in the positions of these meridionals as the monomer ratio is varied.

Keywords X-ray diffraction; liquid crystalline copolyesters; structure determination; random chains; computer modelling

INTRODUCTION

We are using X-ray methods to investigate the physical structure of the high strength fibres prepared from some wholly aromatic copolyesters, *viz.* condensation copolymers of *p*-hydroxybenzoic acid (B), 2,6-dihydroxy naphthalene (N), and terephthalic acid (P), where N and P are present in equal molar quantities[1]. These copolymers can be melt-spun as fibres for proportions of B between 30 and 70 mol %. The melts are liquid crystalline, and this order is retained during spinning, leading to highly oriented high strength fibres. We are analysing the X-ray patterns of these fibres in order to describe the three-dimensional arrangement of the molecules, and our preliminary results are described below. This copolymer system is one of a larger group of melt-spinnable liquid crystalline copolyesters (see for example references 1–13), for which we aim to develop a more general understanding of the structure–property relationships.

At present, relatively little is known about the chemical and physical structures of the B/N/P copolymers: it has yet to be established chemically whether they are truly random copolymers, or whether there is any block copolymer character. In our analyses of the X-ray patterns, we have considered the possibilities of both block and random copolymers. As will be seen, we find no evidence favouring extensive block structures and have proceeded to analyse the data in terms of an assembly of oriented chains of random sequence.

EXPERIMENTAL

Melt-spun copolyester fibres were generously supplied by Celanese Research Corp., Summit, N.J., prepared as described by Calundann[3] for the following B/N/P mole ratios: 60/20/20, 50/25/25, and 40/30/30. The molecular weights are reported to be approximately 22000, corresponding to approximately 150 residues per chain. Specimens for X-ray work were prepared as bundles of parallel fibres. X-ray diffraction patterns were recorded on Kodak no-screen X-ray film using a Searle toroidal focusing X-ray camera and nickel-filtered Cu Kα radiation from a Rigaku-Denki rotating anode X-ray generator. The *d*-spacings were calibrated using calcium fluoride.

Calculation of the axial transform for chains of random sequence

Averaged squared transforms for oriented chains of random sequence were computed for comparison with the meridional intensity distribution. The chemical structure will inevitably lead to a highly extended chain conformation, and it is likely that this feature, together with the stacking of the flat benzene and naphthalene rings of adjacent chains, leads to the liquid crystallinity. A typical random BNP sequence ... P–B–B–N–P–B–N–B– ... is shown in full below.

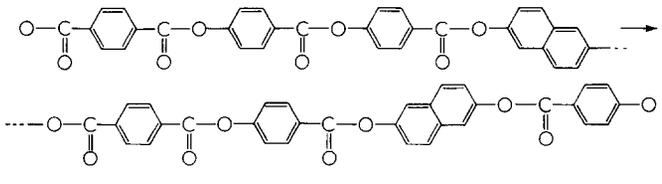

The intensity on the meridian of the X-ray fibre diagram depends on the axial projection of the structure. The bonds linking successive monomers are almost collinear, and hence the axial projection will be almost independent

0032-3861/82/050671-05$03.00

of the rotational conformation (i.e. the relative orientation of the monomers). As a first approximation we have treated the monomers as points along a straight line, positioned for convenience at the ester oxygens. The above chain would be represented as follows:

The oxygen–oxygen distances for the B, N, and P residues were taken as 6.34, 7.75, and 7.15 Å, respectively, based on the single crystal X-ray determinations of the structures of phenyl benzoate[14] and other model compounds[15–17]. The Fourier transform for such an array of points is

$$F(Z)=\sum_{j=1}^{N}\exp(2\pi iZz_j)$$

where z_j is the coordinate of the jth of N points, and Z is the reciprocal space coordinate.

B,N,P permutations were produced using a random number generator, taking into account the B/N/P ratio, the allowed chemical combinations, and depletion of the monomer supply. The observed intensity $I(Z)$ can be compared (qualitatively) with $F^2(Z)$ following averaging over a sufficiently large number of chains to model a random structure.

$$F^2{}_{av}(Z)=\frac{1}{n}\sum_{i=1}^{n}F_i{}^2(Z)$$

where $F_i^2(Z)$ is the squared Fourier transform for the ith of n chains. In our calculations we have averaged $F^2(Z)$ for 250 chains, each of 40 monomers, from $Z=0$ to 1/1.5 Å^{-1} in 500 increments. The averaged transform was then smoothed three times by taking the arithmetic average of ten neighbouring points for each value of Z. The resulting curve was not affected appreciably by the use of a larger number of chains or longer chains. (It is possible that the length of the calculation can be reduced by convolution of functions describing the monomer distributions, and we are currently investigating these possibilities.)

RESULTS AND DISCUSSION

X-ray fibre diagrams

The X-ray fibre diagrams for the three fibre preparations are shown in *Figures 1a–c*. In view of the difficulties in reproduction, schematics of these patterns are shown in *Figures 2a–c*.

The patterns are characterized by broad intense non-Bragg scatter in the equatorial region at $d=6$–3 Å, plus weaker diffuse maxima off the equator, as indicated in *Figure 2*. In addition there are some sharper maxima that can be classified as follows.

(i) All three fibre diagrams show intense equatorials at $d=4.43$ Å and 2.57 Å, and an intense off-equatorial at $d=3.26$ Å.

(ii) Three strong meridionals are observed, two in the region of $d=3$ Å, and one at $d\simeq 2$ Å; the actual d-spacings are shown in *Table 1*, and they are significantly different across the three patterns. In particular the separation between the first two maxima decreased from 0.52 to 0.33 Å as the proportion of B increases from 40 to 60%. At the same time the intensity of the second maximum increases relative to the first. It is also interesting that the second maximum is appreciably sharper than the first. In addition to these three maxima there is more diffuse meridional intensity in the region of $d=2.3$ Å.

(iii) There are some weak meridional and off-meridional maxima in the region of $d>5$ Å; there are also some continuous rings in the same region. All of these features are not common to the three patterns. The sharpness of

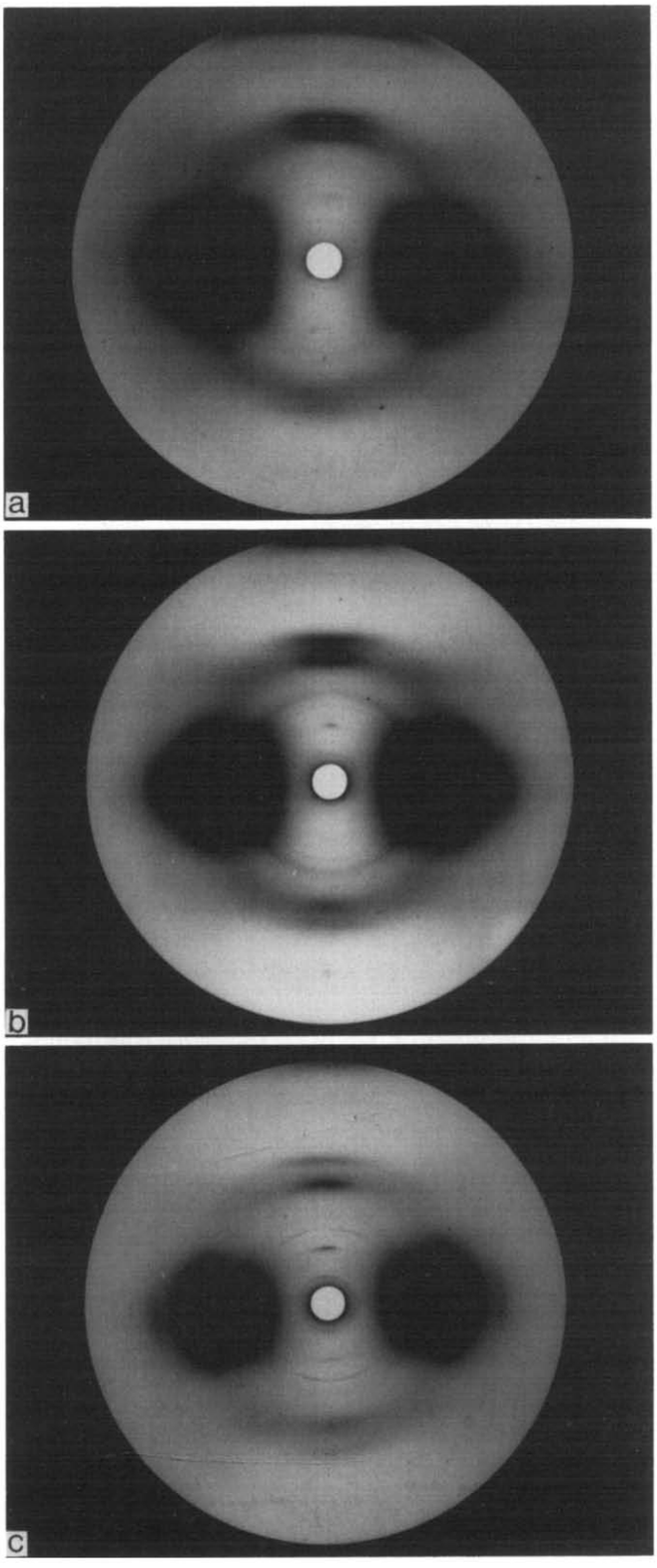

Figure 1 X-ray diffraction patterns of fibres with different B/N/P ratios: (a) 60/20/20; (b) 50/25/25; (c) 40/30/30. The fibre axis is vertical except that the fibres are tilted slightly from the plane perpendicular to the beam

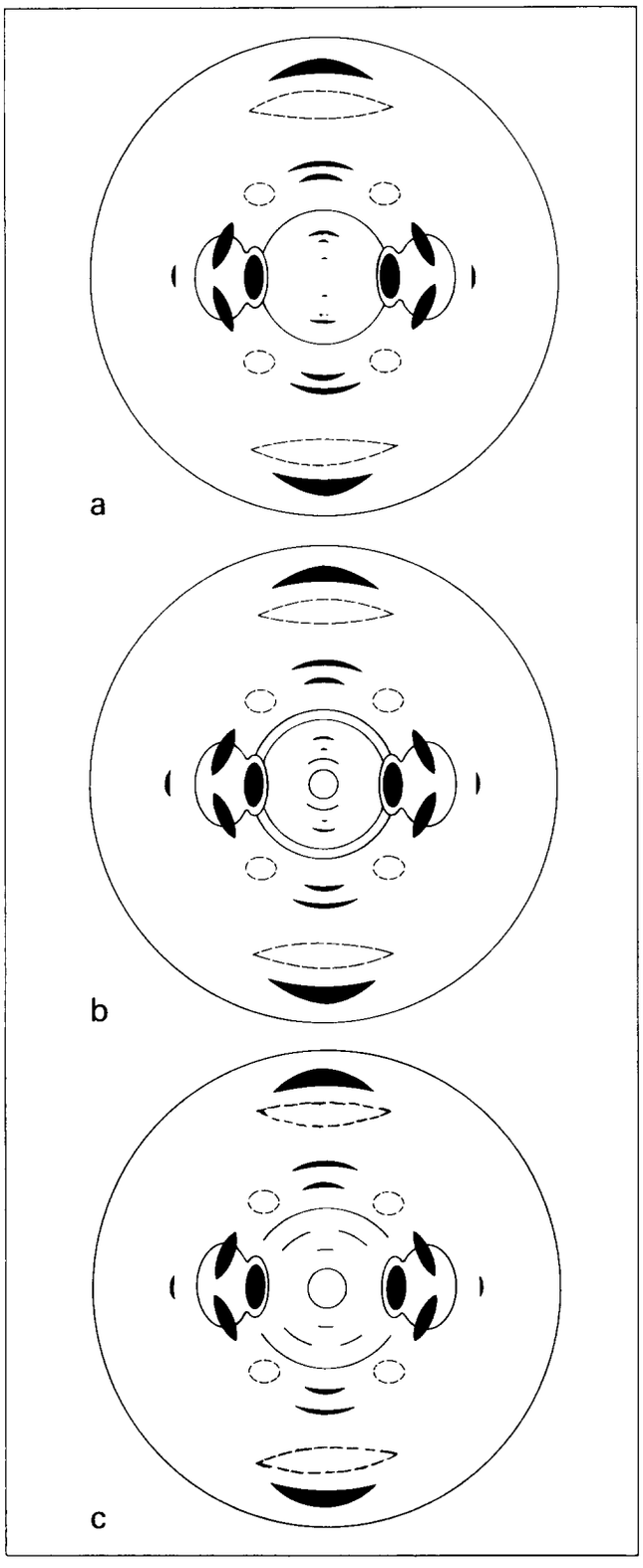

Figure 2 Schematics of the X-ray patterns of fibres with different B/N/P ratios shown in *Figure 1*. (a) 60/20/20; (b) 50/25/25; (c) 40/30/30. The extent of intense non-Bragg scatter on the equator is indicated by the solid lines

some of the reflections suggests that they are Bragg reflections from some relatively large crystallites. The *d*-spacings of the meridionals are given in *Table 1*, and they appear to be multiples of one or both of the spacings in the 3 Å region.

The intense broad equatorial scatter, together with the relatively well defined meridional maxima are characteristic of a highly oriented (parallel) array of polymer chains, that are otherwise poorly packed together due to axial shifts and stacking faults, as has been considered previously for liquid crystalline fibres by Wendorff[18]. Such diffraction features would be expected for parallel chains of random sequence, but could also arise for distorted block copolymer structures. However, in the latter case, the poly(B) and poly(N–P) blocks would each have their own contribution to the pattern, which would be at constant *d*-spacing but would have different relative intensities for different monomer proportions. The variability in *d*-spacing of the observed meridional intensities is inconsistent with this explanation based on oriented blocks. Another possibility is that blocks of poly-(B) could be responsible for the meridionals at $d \simeq 6.0$, 3.0, and 2.0 Å. However, this would not necessitate extensive block copolymer structure since the truly random copolymer is predicted to contain appreciable $(B)_n$ sequences, especially the 60/20/20 preparation for which the meridionals at 6.05, 2.98, and 2.01 Å are the most intense.

The strong equatorial and off-equatorial reflections are constant features of the three patterns and probably arise from stacking of the benzene and naphthalene rings. It is likely that even fully random chains will have extended ribbon-like conformations that are able to stack together, and this property is probably important in developing liquid crystallinity in the melt. Some of the weak inner reflections are remarkably sharp and must arise from relatively large crystallites. It is possible that some of these reflections arise from truly crystalline blocks, but if so these structures constitute only a small fraction of the total polymer. Certain reflections are highly arced or continuous rings indicating a low degree of orientation, which is inconsistent with the high orientation demonstrated by the rest of the pattern. It is possible that these sharp weak arced reflections are due to a poorly

Table 1 *d*-Spacings of observed and calculated meridional maxima

B/N/P ratio	Observed from fibre diagrams (Å)	Calculated transform peaks (Å)
60/20/20	~6.8 (weak, diffuse)	6.757
	6.05 ± 0.05 (weak)	
	3.31 ± 0.03 (strong)	3.394
	2.98 ± 0.03 (strong)	3.086
	~2.3 (broad, diffuse)	2.239 (broad)
	2.01 ± 0.03 (very strong)	2.119
		2.005
		1.616
50/25/25	6.98 ± 0.07	6.881
	~5.9 (weak, diffuse)	
	3.38 ± 0.03 (strong)	3.456
	2.97 ± 0.03 (strong)	3.074
	~2.3 (broad, diffuse)	2.336 (broad)
	2.02 ± 0.03 (very strong)	2.112
		1.903
		1.623
40/30/30	6.96 ± 0.05 (weak)	7.009
	3.48 ± 0.03 (strong)	3.521
	2.96 ± 0.03 (strong)	3.049
	~2.3 (broad, diffuse)	2.427 (broad)
	2.00 ± 0.03 (strong)	2.125
		1.928
		1.630

A few extremely weak maxima are also seen at higher *d*-spacing for each B/N/P ratio

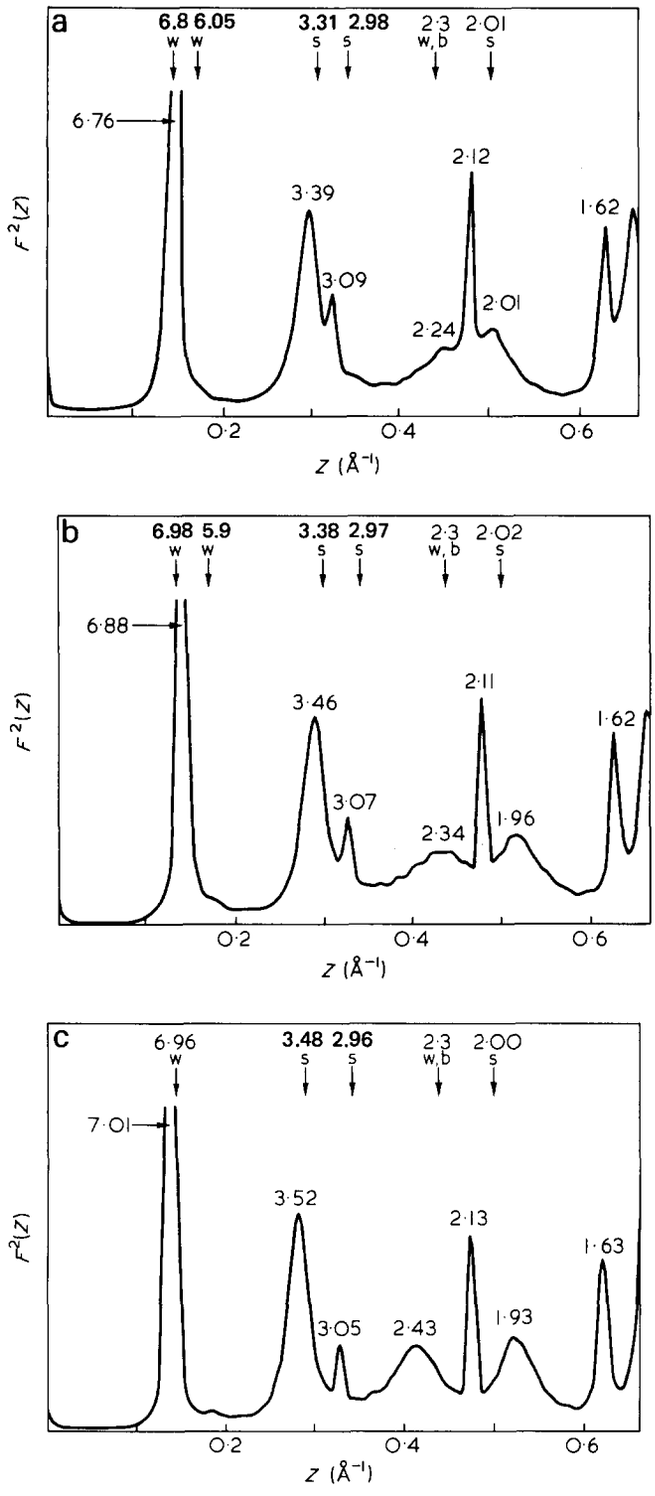

Figure 3 Squared averaged smoothed Fourier transforms of point models for random chains of the following B/N/P ratios. (a) 60/20/20; (b) 50/25/25; (c) 40/30/30. The positions of the observed meridional maxima are indicated by the vertical arrows; the intensities are indicated by s = strong, w = weak, b = broad. The *d*-spacings of the observed and calculated maxima are given in Å units. $F^2(Z)$ is on a linear relative scale

oriented crystalline impurity, such as a low molecular weight reaction product.

Thus the major features of the pattern are consistent with a structure consisting of parallel chains of random sequence. The diffraction characteristics of such a structure have not been considered previously, and we have proceeded to set up random chain models and to compute the predicted diffraction patterns. As a starting point we have considered the meridional intensities to see whether we can reproduce the variability of the *d*-spacings using the random chain model.

Computed axial transforms

The averaged squared Fourier transforms for the point sequences corresponding to the three monomer ratios are shown in *Figures 3a–c*. The *d*-spacings of the peaks are indicated and the positions of the observed meridional intensities are shown by the arrows; the observed and calculated *d*-spacings for the peaks are also listed in *Table 1*. In comparing the observed and calculated data, only the positions of the peaks (i.e. the *d*-spacings) are important. The effect of intra-residue interference needs to be introduced through the use of a full atomic model for the chain before we can compare intensities, but this should have relatively little effect on the positions of the predicted maxima.

The three calculated transforms are not identical but have the same basic features: a single peak at $d \simeq 6.9$ Å, a doublet in the region $d = 3.6$–3.0 Å, a broad peak in the region $d = 2.4$–2.2 Å, and a sharp peak at $d \simeq 2.1$ Å. The similarity continues at $d < 2$ Å, but this is outside the range of the observed meridional data and will not be considered further.

Given the simplicity of the model, the agreement between the observed and calculated data is remarkable. The positions of the two calculated peaks in the 3 Å region and the single peak at 2.1 Å are within 0.1 Å of the observed *d*-spacings for the three strong reflections for each pattern. The calculations reproduce the closing of the gap between the two peaks in the 3 Å region with increasing proportion of B: the calculated separation decreases from 0.47 Å to 0.39 Å to 0.30 Å as compared to the observed decrease from 0.54 Å to 0.43 Å to 0.33 Å respectively, for the three specimens. In addition, the second of these peaks is sharper than the first, as is observed. The predicted peak at $d \simeq 6.9$ Å is broad enough to include the weak meridional maxima in this region. The calculated high intensity should be reduced considerably when the full atomic model is considered, i.e. when we allow for interference between atoms in the same residue. Finally the broad peak at $d \simeq 2.4$–2.2 Å matches the diffuse meridional intensity observed in this region for all three monomer ratios.

The agreement obtained indicates that we can reproduce the important features of the meridional data by a point model for oriented chains of random sequences. The match between the observed and calculated *d*-spacings for the three strong (observed) meridionals is already very good but could be improved by making small reductions in the lengths or axial increments for the three monomer units, i.e. by use of slightly different geometry for the chain than has been assumed in the present model. We are now extending these calculations to atomic models for the chains. There is no information at present with regard to the reactivities of the monomers, and we have worked with equal reactivity ratios. However we do have the capability to vary the reactivity ratios in the program used to set up the monomer sequences, which will allow introduction of block copolymer character. Use of the full atomic model will also allow us to consider packing of the chains, and hence to predict the entire X-ray pattern.

ACKNOWLEDGEMENTS

We thank Drs S. Sprague, I. Hay, and M. Jaffe of Celanese Research Corp., Summit, N.J., for supplying the specimens and for their helpful discussions. This research is supported by NSF through Materials Research Laboratory grant No. DMR78-24150 and also grant No. DMR81-07130 from the Polymers Program.

REFERENCES

1 Calundann, G. W. (Celanese), US Pat. 4067852 (1978)
2 Calundann, G. W., Davis, H. L., Gorman, F. J. and Mininni, R. M. (Celanese), US Pat. 4083829 (1978)
3 Calundann, G. W. (Celanese), US Pat. 4184996 (1980)
4 Calundann, G. W. (Celanese), US Pat. 4130545 (1978)
5 Warner, S. B. *Macromolecules* 1980, **13**, 450–452
6 Kuhfuss, H. F. and Jackson, W. J. (Tennessee Eastman), US Pat. 3804805 (1974)
7 Jackson, W. J. and Morris, J. C. (Tennessee Eastman), US Pat. 4181792 (1980)
8 Jackson, W. J. and Kuhfuss, H. F. *J. Polym. Sci., Polym. Chem. Edn.* 1976, **14**, 2043–2058
9 Cottis, S. G., Economy, J. and Nowak, B. E. (Carborundum), US Pat. 3637595 (1972)
10 Volksen, W., Dawson, B. L., Economy, J. and Lyerla, J. R. *Polym. Prep.* 1979, **20(1)**, 86–89
11 Schaefgen, J. R. (du Pont), US Pat. 4118372 (1978)
12 Goodman, I., McIntyre, J. E. and Stimpson, J. W. (I.C.I), US Pat. 3321437 (1967)
13 Preston, J. Synthesis and Properties of Rodlike Condensation Polymers in 'Liquid Crystalline Order in Polymers', (Ed. A. Blumstein), Academic Press, New York (1978)
14 Adams, J. M. and Morsi, S. E. *Acta Cryst.* 1976, **B32**, 1345–1347
15 Rajan, S. S. *Acta Cryst.* 1978, **B34**, 998–1000
16 Bailey, M. and Brown, C. J. *Acta Cryst.* 1967, **22**, 387–391
17 Colapietro, M. and Domenicano, A. *Acta Cryst.* 1978, **B34**, 3277–3280
18 Wendorff, J. H. Scattering in Liquid Crystalline Polymer Systems in 'Liquid Crystalline Order in Polymers', (Ed. A. Blumstein), Academic Press, New York (1978)